

# Analog-antianalog isospin mixing in $^{47}\text{K}$ $\beta^-$ decay

Brian Kootte<sup>1</sup>, H. Gallop<sup>1,2</sup>, C. Luktuke<sup>1,2</sup>, J.C. McNeil<sup>3,1</sup>, A. Gorelov<sup>1</sup>,  
D. Melconian<sup>4</sup>, J. Klimo<sup>4</sup>, B.Vargas-Calderon<sup>4</sup>, and J.A. Behr<sup>1,3\*</sup>

<sup>1</sup>TRIUMF, 4004 Wesbrook Mall,  
Vancouver, BC V6T 2A3 Canada

<sup>2</sup>U. Waterloo

<sup>3</sup>U. British Columbia

<sup>4</sup>Cyclotron Institute, Texas A&M

(Dated: February 9, 2024)

The decay widths of isobaric analog resonances are modelled well by analog-antianalog isospin mixing via the Coulomb interaction. However, the effects of isospin mixing of the antianalog on nuclear beta decay angular correlations are generally measured to be much smaller than predicted by analog-antianalog. We have measured the isospin mixing of the  $I^\pi = 1/2^+$   $E_x = 2.8$  MeV state in  $^{47}\text{Ca}$  with the isobaric analog  $1/2^+$  state of  $^{47}\text{K}$ . Using the TRIUMF atom trap for  $\beta$  decay, we have measured a nonzero asymmetry of the emitted  $^{47}\text{Ca}$  with respect to the initial  $^{47}\text{K}$  spin polarization, which supported by the beta asymmetry implies a nonzero ratio of Fermi to Gamow-Teller matrix elements  $M_F/M_{GT} = -0.096 \pm 0.037$ . Interpreting as mixing between this state and the isobaric analog state implies a Coulomb matrix element of  $72 \pm 29$  keV. The latter is an order of magnitude larger than observed on  $\beta$  asymmetry measurements in similar decay systems, which we attribute to the simplicity of  $^{47}\text{K}$  and  $^{47}\text{Ca}$  states near doubly-closed shells, and thus a relatively unfragmented antianalog configuration. The result supports pursuing a search for time-reversal odd, parity-even, isovector interactions using a correlation in  $^{47}\text{K}$   $\beta$  decay.

## I. INTRODUCTION

The neutron beta decays to its isobaric analog state, the proton, as does tritium. Many other isotopes undergo beta minus decay to states of same spin  $I$  and parity  $\pi$ , but because of the extra Coulomb energy at higher  $Z$ , decay to the isobaric analog state is energetically forbidden. So the Gamow-Teller operator dominates, while the Fermi operator linking isobaric analog states is only allowed if some low-lying final state of same  $I\pi$  is mixed by an isospin-breaking interaction with the excited isobaric analog. We see such isospin breaking in an  $I^\pi = 1/2^+$  state in the  $^{47}\text{Ca}$  nucleus 80% fed by the beta decay of  $^{47}\text{K}$ . Interference between Gamow-Teller and isospin-suppressed Fermi amplitudes produces a small asymmetry of the progeny recoil direction with respect to the initial nuclear spin, which we measure with TRIUMF's Neutral Atom Trap for beta decay (TRINAT). Our result below from a weighted average of recoil and beta asymmetries is  $M_F/M_{GT} = -0.096 \pm 0.037$ , implying a Coulomb mixing matrix element  $72 \pm 26$  keV, an order of magnitude larger than measured in other beta asymmetry measurements in nearby nuclei.

Since  $^{47}\text{Ca}$  and  $^{47}\text{K}$  are near closed shells, that single known  $^{47}\text{Ca}$   $1/2^+$  state may contain much of the antianalog configuration and its predicted 190 keV mixing matrix element with the analog [1]. Sensitivity to time reversal-odd parity-even (TOPE) inherently isovector [2] N-N interactions through a beta-nu-spin correlation is thought to be enhanced in these systems, as they are referenced to Coulomb rather than strong interactions [3],

while in this  $^{47}\text{K}$  decay case the nuclear matrix elements of such an isovector TOPE interaction may also escape fragmentation.

## II. THEORY AND METHODS

### A. Isospin-forbidden $\beta$ decay

In the angular distribution for allowed  $I=1/2$   $\beta$  decay [4]:

$$dW = F(E, Z) p E p_\nu E_\nu \left( 1 + a \frac{\vec{p}_\beta \cdot \vec{p}_\nu}{E_\beta E_\nu} + \hat{I} \cdot (A_\beta \frac{\vec{p}_\beta}{E_\beta} + B_\nu \frac{\vec{p}_\nu}{E_\nu}) \right), \quad (1)$$

isospin-suppressed Fermi decay alters the correlation coefficients from their Gamow-Teller values:

$$a = 1 \dots; A = A_{GT} + f(M_F); B = -A_{GT} + f(M_F) \quad (2)$$

with  $f(M_F) = \sqrt{\frac{J}{J+1}} M_F/M_{GT}$ . The recoil asymmetry is then proportional to  $A+B$ , which vanishes when  $M_F=0$ . (Analytic expressions for the proportion, possible if the Fermi function is set to unity, are given in Refs. [5, 6]; we compare here entirely to numerical simulations.)

### B. Analog-antianalog mixing

The antianalog configuration has same spin and occupancy of spatial orbitals as the isobaric analog, but has  $T=T_z$  with the antisymmetry of its wavefunction encoded differently between spin and isospin parts so that

\* behr@triumf.ca

is orthogonal to the analog state. Auerbach and Loc [1] using schematic harmonic oscillator wavefunctions write a closed-form expression for analog-antianalog Coulomb mixing,  $\langle \mathcal{A} | H_{\text{Coul}} | \bar{\mathcal{A}} \rangle = 0.35 \frac{\sqrt{n_1 n_2}}{2T} \frac{Z}{A^{2/3}} \text{MeV}$ , where  $n_1$  and  $n_2$  are the number of excess neutrons in two major shells. This deliberately straightforward calculation is then backed by RPA in demonstrative cases to accuracy 20%. In our case of  $^{47}\text{Ca}$ , the closed form expression gives 200 keV.

### C. $^{47}\text{K}$ $\beta^-$ decay to $^{47}\text{Ca}$

The level scheme for  $^{47}\text{K}$  is in Fig. 1. The ground state of  $^{47}\text{Ca}$  is  $7/2^-$ , consistent with fp shell single-particle occupancy—the 2nd-forbidden decay to this state has never been observed. 80% of the decay is known to go to the 2560 keV excited  $1/2^+$  state, 19% to the 2578 keV first excited  $3/2^+$  state, and another 1% is known to decay to several other  $3/2^+$  states [7].

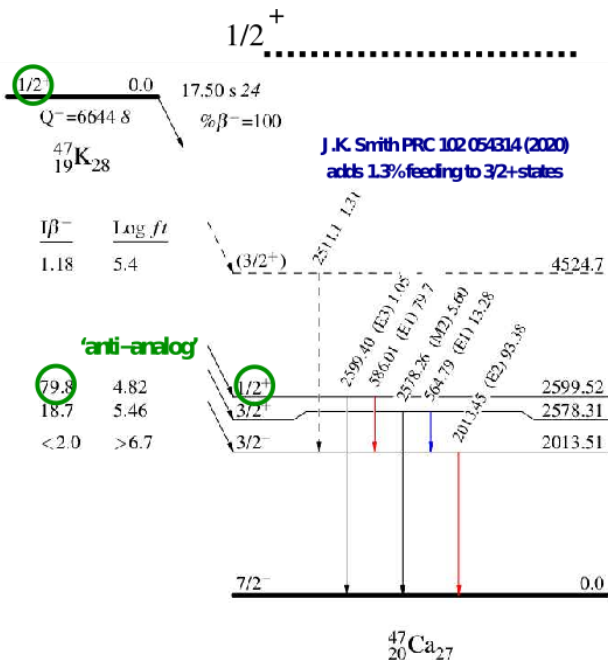


FIG. 1.  $^{47}\text{K}$  decay, modified from ENSDF including info from Ref. [7]

The beta asymmetry is X for  $1/2^+$  and Y for  $3/2^+$  final states for pure GT. The weighted average is  $Z \pm A$ . We include this in our simulation of pseudo  $A_\beta$  below.

### III. EXPERIMENT:

In this section we show experimental details of the atom trapping, the polarization techniques, the detectors (in-vacuum ion and shakeoff electron detection, and

$\beta^-$   $\Delta E$ -E telescopes), the data-taking, and backgrounds from untrapped atoms.

#### A. TRIUMF Neutral Atom Trap

In Fig. 2 we sketch (exported from a GEANT4 simulation, with laser beams superimposed) the detection apparatus of TRIUMF’s Neutral Atom Trap for  $\beta$  decay (TRINAT). Not shown is the collection trap from a vapor cell cube nor the push beams [8].

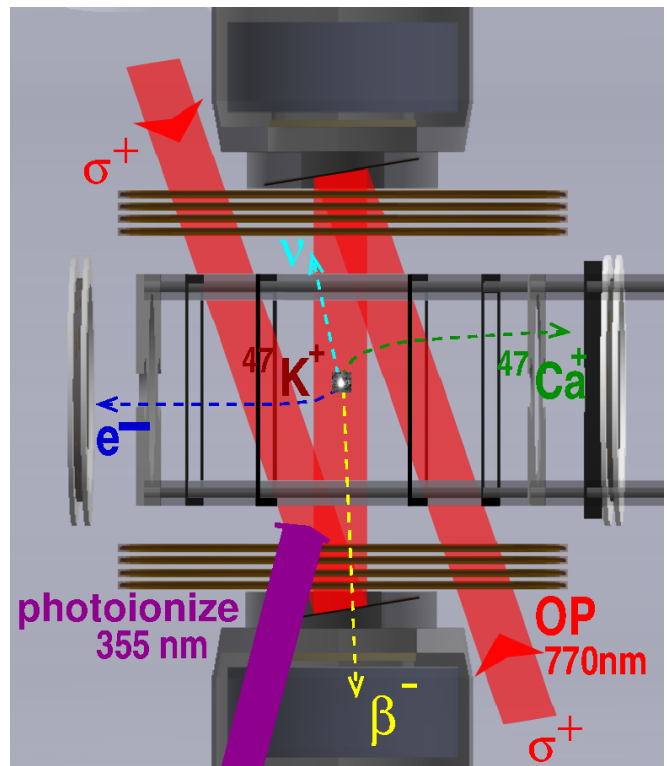


FIG. 2. TRINAT during the optical pumping time. Shown are  $\beta$  telescopes, mirrors for optical pumping light, magnetic field coils, electric field electrodes, and microchannel plates for electron and ion detection. A CMOS camera image of 1,000 trapped atoms is superimposed.

We trapped 500-1,000  $^{47}\text{K}$  atoms over a 16 hr time period. We state here some foibles of our setup that did not compromise our measurement and that, once fixed, should allow us to trap more atoms in the future. We used 250 mW of light from a Ti:Sapph to trap atoms in the collection light, and similarly 200 mW to trap them in the detection trap. This light we found optimized the number of atoms trapped when tuned about 3 linewidths to the red of the  $4S1/2$  to  $4P3/2$   $F=1$  to  $F=2$  transition, as measured with respect to the optical resonance measured by Ref. [9] (using offsets from acousto-optical modulators from a stable potassium saturation spectroscopy reference).

The repumping light on the  $F=0$  to  $F=1$  transition

was about 50 mW from a tapered amplifier laser that was left on in the collection trap. In the detection trap, the repumping light was from the optical pumping beams only, which were left on all of the time. This meant no repumping light at all for the transverse cooling between traps.

## B. Polarization by optical pumping

Details of optical pumping are very similar to our  $^{37}\text{K}$  measurement [10]. Changes include much thinner pellicle mirrors along the optical pumping axis to reduce  $\beta$  straggling, made from 4 micron thick kapton lined with 100 nm of gold. The optical pumping light quality is improved from 0.991 to closer to 0.996 Stokes parameter  $S_3$ .

We alternate 2.9 msec trapping with 1.1 msec optical pumping, during which we make the polarized beta decay measurements. It takes time to switch the magnetic field from the magneto-optical trap (MOT) quadrupole field to a uniform field by reducing currents and flipping one coil.

During the polarization time, we apply circularly polarized light along the quantization axis. Once we start the OP cycle, atoms increase spin to maximum, then stop absorbing in the S1/2 to P1/2 transition used. If light is linearly polarized, atoms keep absorbing, and the atoms and nuclei remain roughly polarized.

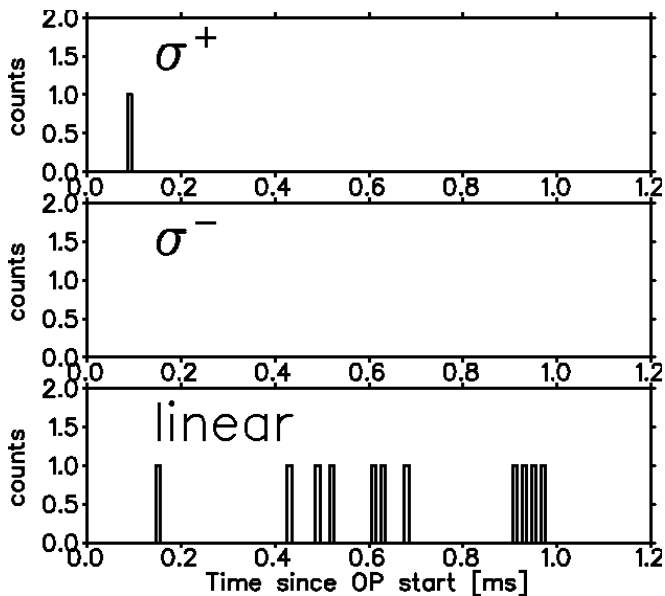


FIG. 3. Excited state population during the optical pumping time for circularly and linearly polarized light. See text for deduction of nuclear polarization.

When excited, 0.5 nsec pulsed from a 355 nm width laser have enough energy/photon to photoionize (a small fraction) of them, detected in the same ion MCP used for the  $^{47}\text{Ca}$  recoils from  $\beta$  decay. The photoions are distin-

guished by their TOF and by their center position. (We determine average trap cloud sizes and positions when the MOT light is on.) In Fig. 3 we show 11 photoions while linearly polarized (in about 1/4? the total time measured) and 1 photon circularly polarized.

For spin-1/2 all the sublevel transitions have equal probabilities, making the deduced nuclear polarization simple to deduce independent of which nearly fully polarized states produce the remaining excited state population. We deduce a fraction of nuclear polarization achieved for the decaying  $^{47}\text{K}$  atoms of  $P = \langle Iz \rangle / I = 0.96 \pm 0.04$ .

We note that the optical pumping light was degrading smoothly in power during the data-taking of both circular and linearly polarized light by a factor of about four, caused by degradation of lithium niobate 3.3 GHz electro-optic modulators from photorefraction at about 4 mW of input optical power. We find from rate equation optical pumping simulations that the ratio of circular to linearly polarized photoions is similar as a function of power, so the average polarization reported reflects accurately the situation. This ratio is also similar as a function of detuning to well within the accuracy we quote, important because we did not determine the resonance location other than optimizing the number of trapped atoms in the MOT.

## C. Detectors

### 1. Ion and Shakeoff electron MCP's

An electric field is formed by a combination of low-Z glassy carbon and titanium electrodes to minimize  $\beta$  scattering. The field is calculated by standard finite element techniques to have average 650 V/cm, and this average is used for simulations. The field collects  $^{47}\text{Ca}$  ions produced in  $^{47}\text{K}$   $\beta^-$  decay to an MCP with 78 mm active area located 10.X cm away. Decay by  $\beta^-$  naturally makes  $^{47}\text{Ca}^{+1}$  ions. Additional low-energy atomic shakeoff electrons, which take on average 6 nsec to reach the opposite 40 mm diameter MCP, trigger time-of-flight (TOF) for  $^{47}\text{Ca}^{+2}$  and higher.

### 2. DSSSD details

Critical to the  $\beta$  asymmetry is discriminating  $\beta$ 's from  $\gamma$ 's, because the production ratio is about 1:2, using. We use the same 0.30 mm thick double-sided silicon strip detectors as Ref. [11], though calibrations have changed with time and with the installation of SiPM readout for our plastic scintillators characterized in Ref. [12].

A cut was therefore made using the energy deposited on the vertical and horizontal strips of the DSSSD located in front of each of the beta scintillation detectors... The same DSSSD energy cut was applied for events triggered from either the top or bottom scintillator and for

all polarizations. By imposing a lower limit ( $>20$ ) on the largest pulse of both horizontal and vertical strips and requiring that the signal on each set of strips not differ by  $>30$ , it was possible to reject all background events from 60 minutes of data recorded with trapped atoms being released to the trap walls.

We show a typical  $E_x$  vs.  $E_y$  plot in Fig.4

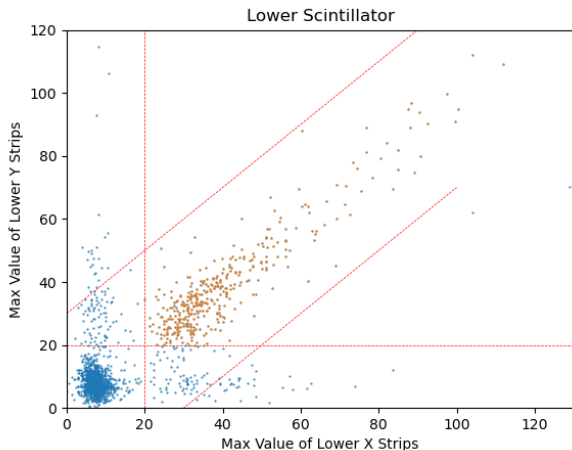


FIG. 4. An additional cut using energy deposited on horizontal and vertical strips of the DSSSD provided the necessary suppression of background to extract the  $\beta$ -asymmetry. The gold coloured points requiring both X and Y strips to have  $Y_i > X+30$  and  $Y_i > X-30$  were retained in the analysis. Most of the background comes from low energy events on each of the strips.

## IV. RESULTS

Here we show results of 12 hours of beamtime, using  $6 \times 10^6/s$  mass-separated  $^{47}\text{K}$  delivered from the TRIUMF/ISAC ISOL-type facility.

### A. $e^-$ -ion MCP coincidences

Our main channel is ion MCP wrt shakeoff electrons produced by charge states  $2+$  and higher. The TOF spectrum Fig. ?? shows  $+2$  to  $+4$  are the main contributions. Their asymmetry wrt to polarization axis is shown to be nonzero in Fig. ??, directly implying a nonzero Fermi contribution to the  $1/2^+ \rightarrow 1/2^+$  transition.

We model this by a numerical integration including one 2 MeV gamma emitted. The result is  $M_f/M_{gt} = -0.102 \pm 0.041$

#### 1. Backgrounds from untrapped atoms.

$t_{1/2} = 19$  sec and trap half-life 10 sec implies more than half the atoms decay after leaving the trap. We have

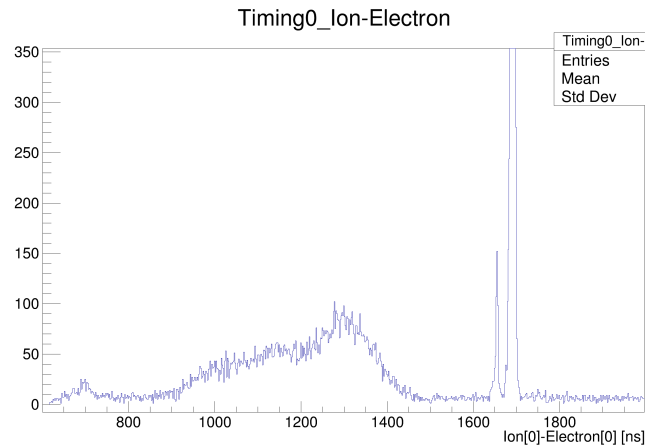


FIG. 5. Time-of-Flight (TOF) of  $^{47}\text{Ca}$  ions triggered by shakeoff  $e^-$ . Needs photoion cut; overlay with sim??

measured this background with 1 hr of data deliberately ejecting atoms from the trap. We deduce a background of  $6 \pm 4\%$  of the events in the  $e^- - ^{47}\text{K}$  channel roughly flat in TOF in the region we use of  $+2, +3$ , and  $+4$  charge states, and include that background in our simulation. This is consistent with a small fraction of the untrapped atoms sticking to the glassy carbon electrodes slightly farther away from the trap– shakeoff electrons from other surfaces are excluded from the electron MCP by the electric field. Our  $\beta$  collimation is sufficient that we see backgrounds consistent zero for the  $\beta$ -recoil channel considered next.

### B. $\beta$ -recoil coincidences pseudo $A_\beta$

We also measure  $\beta$ 's in coincidence with  $^{47}\text{Ca}$  recoils. If we measured  $^{47}\text{Ca}$  recoils over all directions and momenta, this would be a measurement of the beta asymmetry. However, some  $^{47}\text{Ca}$  escape the MCP, perturbing the asymmetry of  $\beta$ 's in coincidence by a well-defined combination of the  $\beta$ - $\nu$  correlation and the  $\nu$  asymmetry.

This observable, which we name pseudo  $A_\beta$ , we also model by numerical integration, including the effects of a single 2 MeV  $\gamma$ . The results are in Fig. 7. Numerical simulations for three values of  $M_f/M_{gt}$  are shown to show sensitivity, along with the best fit. A single straight line for  $M_f=0$  and hypothetical full collection of  $^{47}\text{Ca}$  is

TABLE I. Systematic uncertainties for  $A_{\text{recoil}}$

Source	Uncertainty
Z fit range	0.012
bkg $6 \pm 4\%$	0.014
Polarization $0.96 \pm 0.04$	0.004
Branching ratio	negligible
Fit Statistics	0.037
Total	0.041

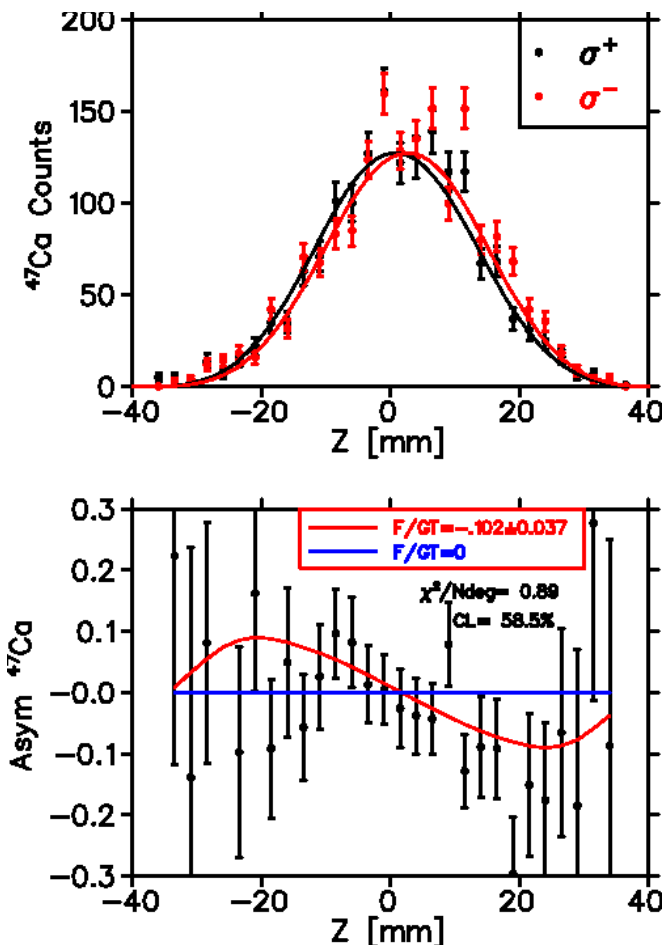


FIG. 6. Top: Distribution of shakeoff  $e^-$  coincidences with  $^{47}\text{Ca}^{+2,3,4}$  recoils along  $Z$ , the polarization axis, for the two polarizations. Bottom: The asymmetry of these distributions, i.e. the difference divided by the sum of the Top distributions. The nonzero asymmetry directly implies a nonzero Fermi contribution.

shown, to indicate how the asymmetries are distorted from  $A_\beta$  from restrictions on the  $^{47}\text{Ca}$  detection. The significantly smaller difference in asymmetry for positive vs. negative  $Z$  is due to an 0.5 mm displacement in the trap position along the  $Z$ -axis and subsequent change in  $^{47}\text{Ca}$  collection, and is well-reproduced by the simulation.

We note that the sign of  $A_\beta$  is determined from this observable. We use this to determine the sign of our spin polarization, as we do not measure the absolute handedness of circularly polarized light.

To deduce a Fermi contribution from pseudo $A_\beta$  requires more precision and accuracy than  $A_{\text{recoil}}$ , because we must distinguish between the experimental value and the nonzero theoretical value for a pure Gamow-Teller transition. E.g., the average coefficient of  $A_\beta$  for  $^{47}\text{K}$  for pure Gamow-Teller transitions is  $-0.467 \pm 0.07$ , where the uncertainty is from the literature branching ratio  $80 \pm 2.0\%$  [7].

The uncertainties are summarized in Table II. The po-

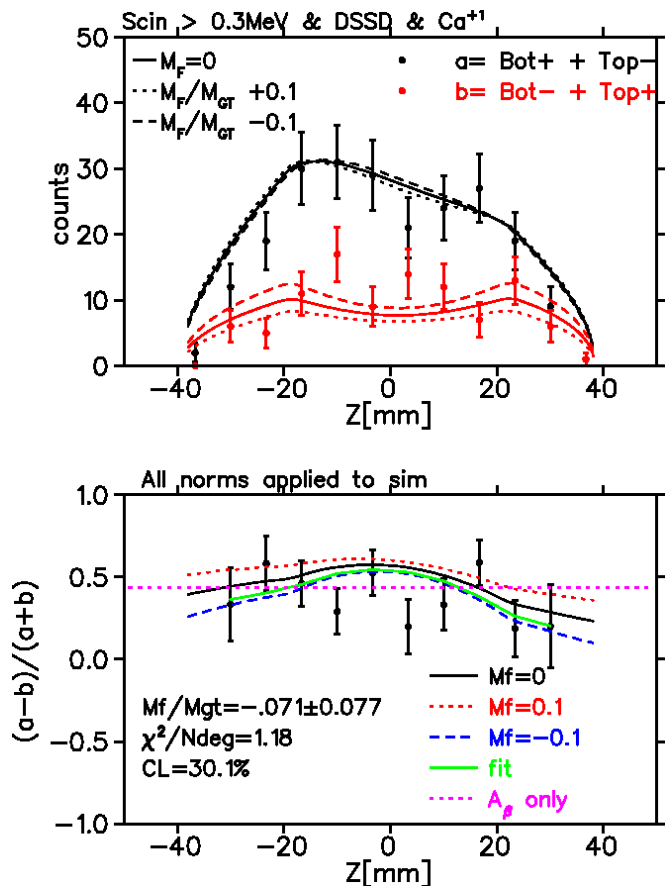


FIG. 7. Similar to Fig. 2, but for  $\beta$ - $^{47}\text{Ca}^{+1,2,3,4}$  coincidences.

larization uncertainty contributes. Based on our previous  $^{37}\text{K}$   $A_\beta$  measurement [11], we scale our experimental value by  $1/1.023$  to approximately account for backscatter, assigning here a more generous uncertainty here of 20% because we have not done full simulations of geometry changes.

The result for  $M_f/M_{gt}$  is  $X$ . It is consistent in sign with the recoil observable, but with larger uncertainty.

TABLE II. Systematic uncertainties for  $\beta$ -recoil coincidences

Source	Uncertainty
Polarization	0.023
Backscatter correction $-0.012 \pm 20\%$	0.0024
E field	0.025
Branching ratios	?
Fit statistics	0.077
Weak Magnetism	0.005?
Total	0.084

### 1. Recoil order corrections.

These we can handle approximately for this nonprecision measurement. Assuming the wavefunction of ini-

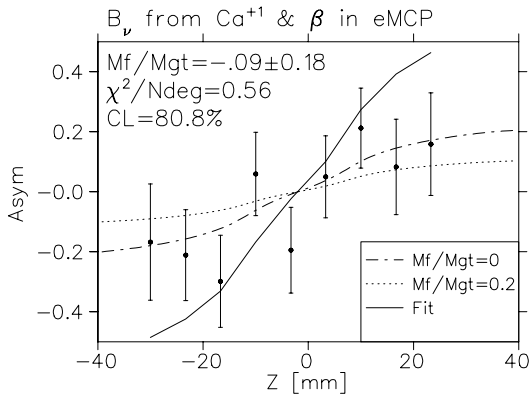


FIG. 8.  $B_\nu$  from using the electron MCP as a  $\beta$  detector. See text.

tial and final  $1/2^+$  states is purely an  $s_{1/2}$  nucleon, the weak magnetism has no orbital correction and becomes the nucleon value, and the first-class induced tensor vanishes. For the 20% branches to  $3/2^+$  states, we further assume the final  $3/2^+$  states are dominated by  $d_{3/2}$ , and use the single-particle expression for weak magnetism for Gamow-Teller transitions (see e.g. Ref. [13]). The result is a correction of less than 0.01 for  $A_\beta$ ??,

## 2. Use of shakeoff electron MCP as a $\beta$ detector

The TOF spectrum 5 shows events in time with  $^{47}\text{Ca}^{+1}$ , but since +1 is the charge state from  $\beta^-$  decay without atomic shakeoff, the electron MCP must be being fired by some other prompt radiation. From coincidence and singles rates we estimate the electron MCP's efficiency for these prompt- $^{47}\text{Ca}^{+1}$  coincidences to be 65%. Noting previous experience of  $\sim 20\%$  efficiency for such detectors for  $\sim \text{MeV}$   $\beta$ 's [14], and noting there are 2  $\gamma$ 's for each  $\beta$ , we find we can reconcile the asymmetry of these events by assuming  $45 \pm 5\%$  of the prompt events produce no asymmetry (Fig. 8). By considering asymmetry of  $^{47}\text{Ca}^1$  along the perpendicular axis, we can set a 1 sigma first upper limit on the time-reversal correlation D of about 0.1. In some models of TOPE interactions this is already a meaningful result.

## C. Result and Isospin breaking

Our weighted average of  $A_{\text{recoil}}$  and pseudo  $A_\beta$  is then  $M_F/M_{GT} = -0.096 \pm 0.037$  for the  $1/2^+$  to  $1/2^+$  transition.

Given the measured  $\log(\text{ft})$  of 4.82 (which implies  $M_{GT} = 0.30$ ?) we deduce  $M_F = ?$  To compare to other nuclei thought to be dominated by analog-antianalog

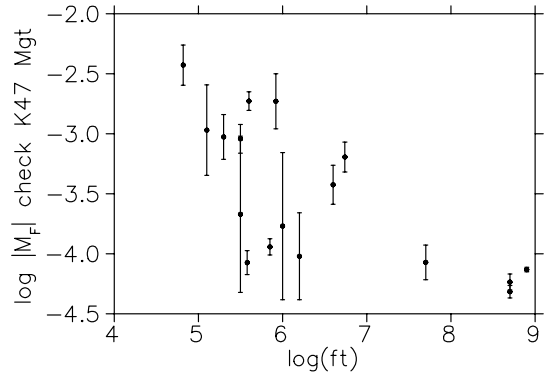


FIG. 9. Isospin-hindered  $\text{Log}(M_F)$  as a function of  $\log(\text{ft})$  from [15]. The present work is at the smallest  $\log(\text{ft})$ .  $M_F$  is falling with complexity of states. JB must check scaling for  $M_F$

mixing, we use a first-order perturbation theory expression from the literature, including the standard ladder operator result for isospin [15, 16]:  $M_F = \frac{\langle A | H_{\text{Coul}} | \bar{A} \rangle}{\Delta E} \sqrt{(T \mp T_z)(T \pm T_z + 1)}$  (upper/lower sign for  $\beta^-/\beta^+$ ) to deduce an effective Coulomb matrix element.  $\Delta E$  is the energy splitting between analog and antianalog?? use lit expr or look it up??. The result is  $H_{\text{Coul}} = -72 \pm 26$  keV.

This matrix element is about 1/3 of the prediction of analog-antianalog mixing. We attribute this to the simple structure of  $^{47}\text{Ca}$ . That it is not the full prediction suggests the state is either more complex than the antianalog or that contributions from other Coulomb mixing mechanisms. Since the antianalog has determined spin equal to the analog, it seems unlikely the antianalog configuration is contained in other states. The sign has physical meaning, and many of the experiments report values less than zero, though Ref. [1] does not calculate the sign.

Most  $\beta$  decay in such systems has much smaller Coulomb matrix elements and  $M_F$ . Fig. 9, a plot of literature measurements of  $M_F$  [15] suggests that modulo an order of magnitude,  $M_F$  is falling with  $M_{GT}$ , i.e. falling with the complexity of nuclear states. This may well be approximately true for many interactions, including TOPE nucleon-nucleon ones. Ref. [3] advocates a TRV measurement in  $^{134}\text{Cs}$ , which has a very large  $\log(\text{ft})$  (and a measurement was similarly pursued in  $^{56}\text{Co}$  [17]), but if matrix elements of nucleon-nucleon interactions [18] are similarly fragmented, a slow Gamow-Teller transition may not be a useful figure of merit for TRV sensitivity.

## V. CONCLUSION

We have measured the ratio of Fermi to Gamow-Teller matrix elements to be  $-0.096 \pm 0.037$ , which implies an relatively large effective Coulomb mixing matrix element  $72 \pm 26$  keV. This is about  $1/3$  the size predicted from

analog-antianalog mixing [1] if the  $1/2^+$  state measured were purely the antianalog configuration. We attribute this larger fraction than typical of analog-antianalog mixing to the existence of the single  $1/2^+$  state in nearly doubly-closed  $^{47}\text{Ca}$ .

- 
- [1] N. Auerbach and M. L. Bui, Coulomb corrections to fermi beta decay in nuclei, *Nuclear Physics A* **1027**, 122521 (2022).
- [2] M. Simonius, Constraints on parity-even time reversal violation in the nucleon-nucleon system and its connection to charge symmetry breaking, *Phys. Rev. Lett.* **78**, 4161 (1997).
- [3] A. Barroso and R. Blin-Stoyle, A test for time-reversal violation in allowed isospin-hindered beta-decay, *Physics Letters B* **45**, 178 (1973).
- [4] J. Jackson, S. Treiman, and H. Wyld, Coulomb corrections in allowed beta transitions, *Nuclear Physics* **4**, 206 (1957).
- [5] J. R. A. Pitcairn, D. Roberge, A. Gorelov, D. Ashery, O. Aviv, J. A. Behr, P. G. Bricault, M. Dombisky, J. D. Holt, K. P. Jackson, B. Lee, M. R. Pearson, A. Gaudin, B. Dej, C. Höhr, G. Gwinner, and D. Melconian, Tensor interaction constraints from  $\beta$ -decay recoil spin asymmetry of trapped atoms, *Phys. Rev. C* **79**, 015501 (2009).
- [6] S. B. Treiman, Recoil effects in  $k$  capture and  $\beta$  decay, *Phys. Rev.* **110**, 448 (1958).
- [7] J. K. Smith, A. B. Garnsworthy, J. L. Pore, C. Andreoiu, A. D. MacLean, A. Chester, Z. Beadle, G. C. Ball, P. C. Bender, V. Bildstein, R. Braid, A. D. Varela, R. Dunlop, L. J. Evitts, P. E. Garrett, G. Hackman, S. V. Ilyushkin, B. Jigmeddorj, K. Kuhn, A. T. Laffoley, K. G. Leach, D. Miller, W. J. Mills, W. Moore, M. Moukadam, B. Olaizola, E. E. Peters, A. J. Radich, E. T. Rand, F. Sarazin, C. E. Svensson, S. J. Williams, and S. W. Yates, Spectroscopic study of  $^{47}\text{Ca}$  from the  $\beta^-$  decay of  $^{47}\text{K}$ , *Phys. Rev. C* **102**, 054314 (2020).
- [8] T. B. Swanson, D. Asgeirsson, J. A. Behr, A. Gorelov, and D. Melconian, Efficient transfer in a double magnetooptical trap system, *J. Opt. Soc. Am. B* **15**, 2641 (1998).
- [9] F. Touchard, P. Guimbal, S. Büttgenbach, R. Klapisch, M. De Saint Simon, J. Serre, C. Thibault, H. Duong, P. Juncar, S. Liberman, J. Pinard, and J. Vialle, Isotope shifts and hyperfine structure of 38–47k by laser spectroscopy, *Physics Letters B* **108**, 169 (1982).
- [10] B. Fenker, J. A. Behr, D. Melconian, R. M. A. Anderson, M. Anholm, D. Ashery, R. S. Behling, I. Cohen, I. Craiciu, J. M. Donohue, C. Farfan, D. Friesen, A. Gorelov, J. McNeil, M. Mehlman, H. Norton, K. Olchanski, S. Smale, O. Thériault, A. N. Vantighem, and C. L. Warner, Precision measurement of the nuclear polarization in laser-cooled, optically pumped 37k, *New Journal of Physics* **18**, 073028 (2016).
- [11] B. Fenker, A. Gorelov, D. Melconian, J. A. Behr, M. Anholm, D. Ashery, R. S. Behling, I. Cohen, I. Craiciu, G. Gwinner, J. McNeil, M. Mehlman, K. Olchanski, P. D. Shidling, S. Smale, and C. L. Warner, Precision measurement of the  $\beta$  asymmetry in spin-polarized  $^{37}\text{K}$  decay, *Phys. Rev. Lett.* **120**, 062502 (2018).
- [12] M. Ozen, J. A. Behr, M. Khoo, F. Klose, A. Gorelov, and D. Melconian, Lineshape response of plastic scintillator to pair production of 4.44 meV  $\gamma$ 's, *Nuclear Instruments and Methods in Physics Research Section A: Accelerators, Spectrometers, Detectors and Associated Equipment* **1055**, 168490 (2023).
- [13] X. B. Wang and A. C. Hayes, Weak magnetism correction to allowed  $\beta$  decay for reactor antineutrino spectra, *Phys. Rev. C* **95**, 064313 (2017).
- [14] A. Gorelov, D. Melconian, W. P. Alford, D. Ashery, G. Ball, J. A. Behr, P. G. Bricault, J. M. D'Auria, J. Deutsch, J. Dilling, M. Dombisky, P. Dubé, J. Fingler, U. Giesen, F. Glück, S. Gu, O. Häusser, K. P. Jackson, B. K. Jennings, M. R. Pearson, T. J. Stocki, T. B. Swanson, and M. Trinczek, Scalar interaction limits from the  $\beta$ - $\nu$  correlation of trapped radioactive atoms, *Phys. Rev. Lett.* **94**, 142501 (2005).
- [15] S. Bhattacharjee, S. Mitra, and H. Padhi, Fermi matrix elements in allowed beta transitions in  $^{56}\text{Co}$ ,  $^{58}\text{Co}$  and  $^{134}\text{Cs}$ , *Nuclear Physics A* **96**, 81 (1967).
- [16] S. D. Bloom, Isotopic-spin conservation in allowed  $\beta$ -transitions and coulomb matrix elements, *Il Nuovo Cimento* **32**, 1023 (1964).
- [17] F. P. Calaprice, S. J. Freedman, B. Osgood, and W. C. Thomlinson, Test of time-reversal invariance in the beta decay of  $^{56}\text{Co}$ , *Phys. Rev. C* **15**, 381 (1977).
- [18] P. Herczeg, The general form of the time-reversal non-invariant internucleon potential, *Nuclear Physics* **75**, 655 (1966).